Detection and Discrimination of Inter-Turn Short Circuit and Demagnetization Faults in PMSMs Based on Structural Analysis

Saeed Hasan Ebrahimi, Martin Choux, and Van Khang Huynh

Department of Engineering Sciences
University of Agder
NO-4879 Grimstad, Norway

Abstract – This paper presents a fault diagnosis method based on structural analysis of permanent magnet synchronous motors (PMSMs), focusing on detecting and discriminating two of the most common faults in PMSMs, namely demagnetization and inter-turn short circuit faults. The structural analysis technique uses the dynamic mathematical model of the PMSM in matrix form to evaluate the system's structural model. After obtaining the analytical redundancy using the over-determined part of the system, it is divided into redundant testable sub-models. Four structured residuals are designed to detect and isolate the investigated faults, which are applied to the system in different time intervals. Finally, the proposed diagnostic approach is numerically verified through a simulation of an inverter-fed PMSM and white Gaussian noise are added to the measured signals from the motor to verify its diagnosis performances.

C.1 Introduction

Nowadays, Permanent Magnet Synchronous Motors (PMSMs) are widely used in different industrial applications owing to their merits of efficiency, power density, and ease of control [1, 2]. The PMSMs in power-trains normally work in harsh working conditions and exposed to various electrical, mechanical, and thermal stresses [3, 4]. These stresses may eventually degrade the insulator in the stator winding, resulting in an inter-turn short circuit (ITSC) fault, or cause the demagnetisation of permanents magnets (PMs) mounted on the rotor assembly [5]. Since ITSC fault involves very few turns, it generates excessive heat, which may result in first efficiency reduction and later in a catastrophic system breakdown if not being diagnosed in time [6]. In addition, PMs used in PMSMs are considered to be not only the most expensive material, but also very sensitive to the stresses [7]. Monitoring and detection of demagnetization in early stages is therefore important in preventing costly down-times and high maintenance costs [8].

Various approaches have been employed to detect ITSC and demagnetization faults in PMSMs. [9, 10] have implemented a signal-based method to investigate the behavior of ITSC and demagnetization faults by monitoring the vibration and temperature in a PMSM. [11, 12] have used data-driven models to detect and classify ITSC and demagnetization faults in a PMSM by using Neural Network. The signal-based and data-driven techniques can effectively detect the faulty case, but they require either advanced sensors or a lot of data for training, without a clear explanation based on physical models. Alternatively, model-based methods are widely employed in the literature [13–15] among which Finite-Element Method (FEM) based models are most recommended due to high analysis accuracy, but they require a deep knowledge of the system, e.g. detailed dimensions and material characteristics [1]. Furthermore, FEM-based models are computational-heavy and are challenging to use in real time. Structural analysis is hence proposed as an alternative solution for detection and isolation of various faults in a complex system, without a prior deep knowledge of the system dynamics [16]. The theory of structural analysis technique has been well developed in the literature [17, 18] and been applied from automotive engine [19], hybrid vehicle [20], to electric drive [16] systems. However, ITSC and demagnetization fault detection and isolation (FDI) for PMSMs is not present in the above-mentioned studies. Investigating sensor faults along with ITSC and demagnetization faults can be challenging especially when it comes to isolation of the sensor faults from ITSC faults since they both add the same fault terms to voltage equations, therefore, sensor measurements are considered not to have any offsets (only noise) and only ITSC and demagnetization faults are studied in this paper.

This paper presents a systematic FDI methodology based on structural analysis for specific investigation of ITSC and demagnetization faults in a PMSM. To accomplish this, a healthy dynamic mathematical model of PMSM in *abc* frame is employed, and specific terms relevant to the presence of ITSC and demagnetization faults are added to the corresponding equations. These added terms include the deviations in the resistance and inductance of the stator winding caused by ITSC fault, and the deviations in the PM linkage flux caused by a demagnetization fault, appearing in the three-phase flux and voltage equations. Further, the analytical redundancy of the model is determined based on the PMSM's structural model. The system is subdivided into smaller over-determined subsystems, in which the faults are detected, and discriminated and four sequential residuals are designed to show the presence of each fault. Eventually, the proposed model is implemented in Matlab/Simulink to verify its effectiveness in different faulty cases with presence of white Gaussian noise in the measured signals.

C.2 Structural Analysis for PMSM under Demagnetization and ITSC Faults

Structural analysis is a model-based technique that can be used in FDI to extract the analytic redundant relations (ARRs) of a system from the mathematical equations describing its dynamic [21, 22]. The structural model is represented by an incidence matrix, in which each row connects an equation to the corresponding unknown variables, known variables, and faults. The analytic redundancy of the system is then obtained through rearranging the rows and columns in a way to form a diagonal structure which is called Dulmage–Mendelsohn (DM) decomposition. From the analytic redundant part of this structure, several smaller over-constrained subsystems can be identified yielding a set of ARRs. Depending on its signature on this set of ARRs, each considered fault might be detected or even discriminated. Subsequently, a few diagnostic tests are designed to inform about the presence of each fault. Here, a structural analysis of a PMSM containing

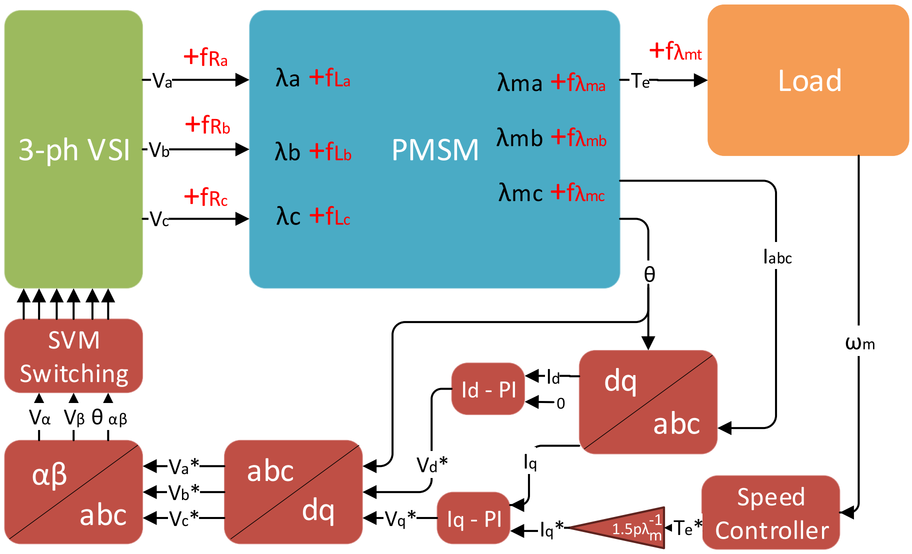

Figure C.1: Modeling diagram of PMSM and drive system.

ITSC and demagnetization faults is presented, and diagnostic tests are proposed for their detection and isolation. Fig. C.1 shows the modeling diagram of faulty PMSM and the drive system components where the parameters are defined below.

C.2.1 PMSM Mathematical Model

The mathematical model of a PMSM with ITSC and demagnetization faults is given by equations $e_1 - e_{12}$ as shown in Eq. (C.1), where v_a, v_b, and v_c are the three phase voltages; i_a, i_b, and i_c are the three phase currents; λ_a, λ_b, and λ_c are the three phase stator flux; λ_{ma}, λ_{mb}, and λ_{mc} are the flux established by PMs in each phase; T_e is the electromagnetic torque, T_L is the Load torque; ω_m is the shaft's angular speed; θ is the electric angular position; R_a, R_b, and R_c are the stator phase resistances and L_a, L_b, and L_c are the stator phase inductances; λ_m is the flux established by PMs; P is the number of poles; J is the rotor inertia, and b is the friction coefficient.

When an ITSC fault appears in one of the phases of motor winding, both resistance and inductance values of that phase is influenced. Here, f_{R_a} and f_{L_a} are added to the corresponding equations of the healthy PMSM to account for ITSC fault in phase-a. Similarly, f_{R_b}, f_{L_b}, f_{R_c}, and f_{L_c} terms are added to account for ITSC faults in phases b and c, respectively.

$$
\begin{aligned}
e1 :& v_a = R_a i_a + \frac{d\lambda_a}{dt} + f_{R_a} \\
e2 :& v_b = R_b i_b + \frac{d\lambda_b}{dt} + f_{R_b} \\
e3 :& v_c = R_c i_c + \frac{d\lambda_c}{dt} + f_{R_c}
\end{aligned}
$$

$$
\begin{aligned}
e4 :& \lambda_a = L_a i_a + \lambda_{ma} + f_{L_a} \\
e5 :& \lambda_b = L_b i_b + \lambda_{mb} + f_{L_b} \\
e6 :& \lambda_c = L_c i_c + \lambda_{mc} + f_{L_c} \\
e7 :& \lambda_{ma} = \lambda_m \sin\theta + f_{\lambda_{ma}} \\
e8 :& \lambda_{mb} = \lambda_m \sin(\theta - 2\pi/3) + f_{\lambda_{mb}} \\
e9 :& \lambda_{mc} = \lambda_m \sin(\theta + 2\pi/3) + f_{\lambda_{mc}} \\
e10 :& T_e = \frac{P}{2}\lambda_m[i_a \cos\theta + i_b \cos(\theta - 2\pi/3) \\
& + i_c \cos(\theta + 2\pi/3)] + f_{\lambda_{mt}} \\
e11 :& \frac{d\omega_m}{dt} = \frac{1}{J}(T_e - b\omega_m - T_L) \\
e12 :& \frac{d\theta}{dt} = \frac{P}{2}\omega_m
\end{aligned}
\tag{C.1}
$$

Further, $f_{\lambda_{ma}}$, $f_{\lambda_{mb}}$, $f_{\lambda_{mc}}$, and $f_{\lambda_{mt}}$ terms are added to equations in case of the demagnetization fault. The known variables are the three-phase voltages and the measurements of currents and angular speed, i.e., y_{v_a}, y_{v_b}, y_{v_c}, y_{i_a}, y_{i_b}, y_{i_c}, and y_{ω_m}, shown in Eq. (C.2).

$$
\begin{aligned}
m1 :& y_{v_a} = v_a, m2 : y_{v_b} = v_b, m3 : y_{v_c} = v_c \\
m4 :& y_{i_a} = i_a, m5 : y_{i_b} = i_b, m6 : y_{i_c} = i_c \\
m7 :& y_{\omega_m} = \omega_m
\end{aligned}
\tag{C.2}
$$

In addition, the mathematical model includes five differential constraints of unknown variables, which are shown in Eq. (C.3).

$$
\begin{aligned}
d1 :& \frac{d\lambda_a}{dt} = \frac{d}{dt}(\lambda_a) \\
d2 :& \frac{d\lambda_b}{dt} = \frac{d}{dt}(\lambda_b) \\
d3 :& \frac{d\lambda_c}{dt} = \frac{d}{dt}(\lambda_c) \\
d4 :& \frac{d\omega_m}{dt} = \frac{d}{dt}(\omega_m) \\
d5 :& \frac{d\theta}{dt} = \frac{d}{dt}(\theta)
\end{aligned}
\tag{C.3}
$$

C.2.2 Structural Model and Analytical Redundancy of the PMSM

The structural model of PMSM with ITSC and demagnetization faults is obtained based on the defined mathematical model in Eqs. (C.1)-(C.3), as shown in Fig. C.2. The incidence matrix contains 24 rows, representing the 12 defined equations in Eq. (C.1), 7 measured known variables in Eq. (C.2), and the 5 differential constraints of unknown variables as shown in Eq. (C.3). The columns of the matrix is subdivided into three groups of unknown variables, known variables, and faults, and each equation is connected to its relevant constraint in any of the three groups through each row. In order to be able to detect and then isolate a fault, it should lie in the structurally over-determined part of

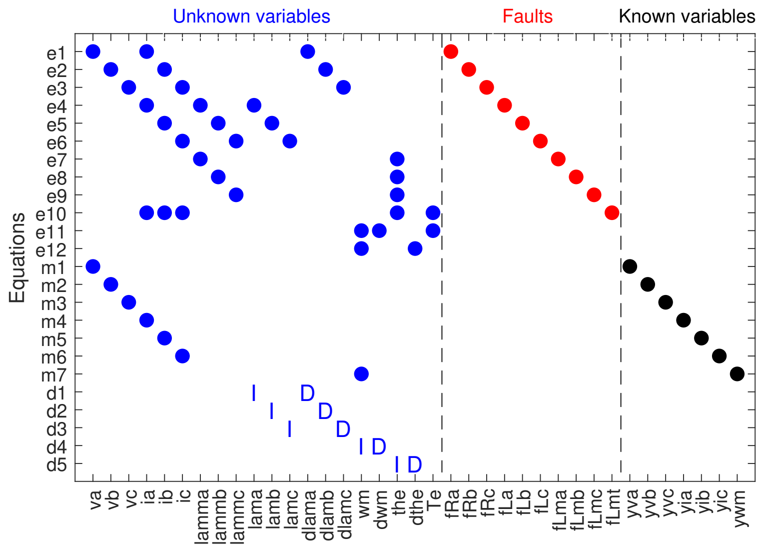

Figure C.2: PMSM structural model.

the model, where there are more equations than unknown variables [18]. To accomplish this, the redundancies of the model are first evaluated by employing DM decomposition tool, which restructures the model into upper triangle shape by rearranging the rows and the columns of the incidence matrix. Fig. C.3 shows the DM decomposition for PMSM structural model, where the analytic redundant part is expressed in the upper left part containing all the faults.

C.3 Diagnostic Test Design

In this section, the procedure of designing diagnostic tests for ITSC and demagnetization faults is discussed. First, the analytic redundant part is divided into smaller redundant subsystems and then sequential residuals are derived to detect each fault.

C.3.1 Finding Testable Sub-Models

Using the algorithm proposed by [23], the system is subdivided into efficient redundant testable sub-models called Minimal Test Equation Supports (MTESs). MTES sets contain specific equations defined in Eq. (C.1), and are found in a way that the considered ITSC (in any of the phases) and demagnetization faults are detected and discriminated. Fig. C.4 shows all the MTES sets found for the considered system here, and Fig. C.5 shows the signature matrix of MTES sets, indicating which faults appear in each MTES. $MTES_1$ includes only $f_{\lambda_{mt}}$ fault term, meaning it can be used for detecting demagnetization fault. $MTES_2$ contains f_{R_c}, f_{L_c}, and $f_{\lambda_{mc}}$ fault terms, therefore, it can be used for detecting ITSC fault in phase c and demagnetization fault. Subsequently, $MTES_3$ can be used for detecting ITSC fault in phase b and demagnetization fault, and $MTES_4$ for detecting ITSC fault in phase a and demagnetization fault.

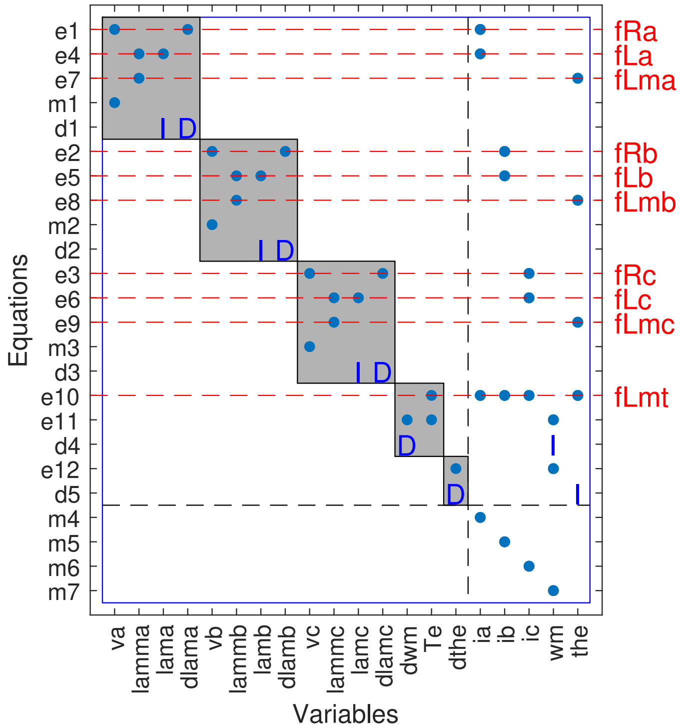

Figure C.3: DM decomposition for PMSM structural model.

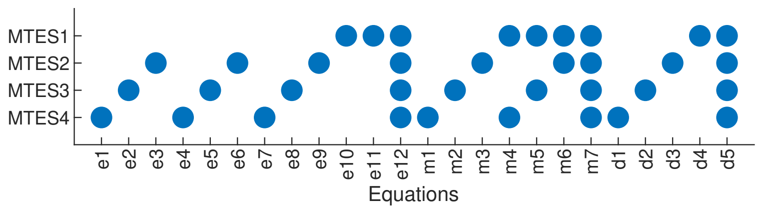

Figure C.4: MTES sets.

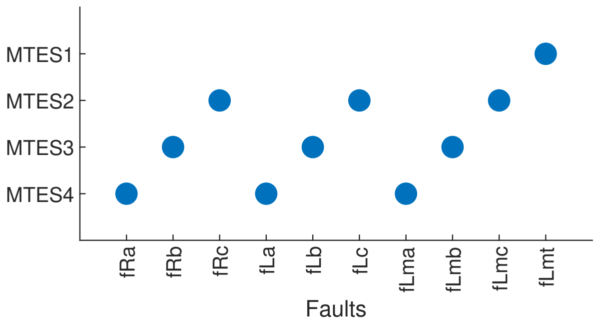

Figure C.5: Fault signature matrix of MTES sets.

C.3.2 Sequential Residuals for Detecting the Faults

In this section, four sequential residuals ($R_1 - R_4$) are derived based on the obtained MTES set. These residuals aim to detect and isolate ITSC fault in phase a, ITSC fault in phase b, ITSC fault in phase c, and demagnetization fault.

1. R_1: $MTES_4$ is used for deriving R_1 based on the difference between measured and calculated voltages of phase a:

$$m1 : R_1 = y_{v_a} - v_a \tag{C.4}$$

   And the sequence of deriving v_a is as follows:

$$\begin{aligned} SV &: \theta = \theta_{state} \\ m7 &: y_{\omega_m} = \omega_m \\ e12 &: \frac{d\theta}{dt} = \frac{P}{2}\omega_m \\ e7 &: \lambda_{ma} = \lambda_m \sin\theta \\ m4 &: i_a = y_{i_a} \\ e4 &: \lambda_a = L_a i_a + \lambda_{ma} \\ d1 &: \frac{d\lambda_a}{dt} = \frac{d}{dt}(\lambda_a) \\ e1 &: v_a = R_a i_a + \frac{d\lambda_a}{dt} \end{aligned} \tag{C.5}$$

   Where θ_{state} is the State Variables (SV) and will be updated after R_1 is calculated as follows:

$$d5 : \theta_{state} = \int d\theta \tag{C.6}$$

2. R_2 and R_3 follow the same procedure mentioned for R_1 to find the difference between measured and calculated phase b and phase c voltages based on $MTES_3$ and $MTES_2$, respectively.

3. R_4: $MTES_1$ is used for deriving R_4 based on difference between the measured and calculated angular speeds:

$$\begin{aligned} e10 : R_4 = T_e - \frac{P}{2}\lambda_m[&i_a \cos\theta + i_b \cos(\theta - 2\pi/3) \\ &+ i_c \cos(\theta + 2\pi/3)] + f_{\lambda_{mt}} \end{aligned} \tag{C.7}$$

Table C.1: Parameters of PM Synchronous Motor

Symbol	Parameter	Value	Unit
V_{dc}	Rated dc bus voltage	320	V
I_s	Rated rms phase current	12.6	A
T_{out}	Output Torque	14	$N.m$
n_s	Rated speed	1200	rpm
R_s	Phase resistance	1.72	Ω
L_q, L_d	Q and D axes inductances	23.3948	mH
J	Rotor inertia	0.00161	$kg.m^2$
b	Rotor damping factor	0.002973	$N.m.s/rad$
λ_m	Flux linkage of PMs	0.1722	
n_s	Pole-pairs	4	

And the sequence of deriving T_e is as follows:

$$\begin{aligned}
SV &: \theta = \theta_{state} \\
m7 &: R_4 = y_{\omega_m} - \omega_m \\
d4 &: \frac{d\omega_m}{dt} = \frac{d}{dt}(\omega_m) \\
e12 &: \frac{d\theta}{dt} = \frac{P}{2}\omega_m \\
e11 &: \frac{d\omega_m}{dt} = \frac{1}{J}(T_e - b\omega_m - T_L) \\
m4 &: i_a = y_{i_a}, m5 : i_b = y_{i_b}, m6 : i_c = y_{i_c}
\end{aligned} \tag{C.8}$$

Where θ_{state} is the state variables and are updated after R_4 is calculated:

$$d5 : \theta_{state} = \int d\theta \tag{C.9}$$

C.4 Simulation and Results

To verify the proposed diagnostic method, a Matlab/Simulink model of a PMSM is implemented based on the model proposed in [24]. Using this model, demagnetization and ITSC faults in any of the three phases can be applied on the PMSM and motor signals under faulty condition can be obtained. The parameters of motor are listed in Table C.1. To test the residual responses under variable operating conditions, the reference for the motor drive's speed controller is set to be variable. Fig. C.6a shows the speed reference and the motor's speed and Fig. C.6b shows the output torque of the motor during the time of the simulation. As can be seen in Fig. C.6a, it takes time for the actual speed of the motor to catch the reference speed (which comes from the controller), since the motor is considered to be stationary in the beginning.

During the simulation, the ITSC and demagnetization faults are applied at different time intervals. At $t = 0.06 - 0.08s$, there appears an ITSC fault in phase a with 5%

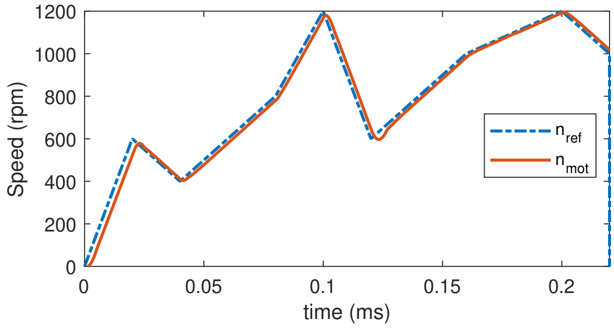

(a)

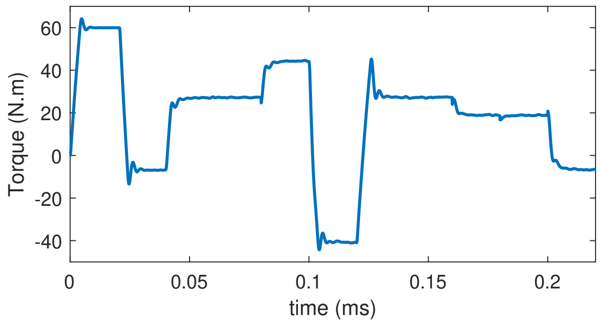

(b)

Figure C.6: Output characteristics of the motor (a) speed, (b) torque.

fault severity (number of shorted turns to total turns in one phase); at $t = 0.1 - 0.12s$, there is an ITSC fault in phase b with 5% fault severity; at $t = 0.14 - 0.16s$, the motor has an ITSC fault in phase c with 5% fault severity; and at $t = 0.18 - 0.2s$, appears a demagnetization fault with 10% fault severity (the flux linkage of PMs is decreased by 20%). To test the effectiveness of the residual responses, a band-limited Gaussian noise is added to the measured values (known variables) here. Without the noise, the residuals can be triggered by any small abnormality in the system and therefore, the diagnostic system can theoretically detect faults with very low severity (e.g. 0.1%) which is not plausible in reality. As mentioned before, the severity of ITSC faults in any of the phases and demagnetization fault are set to 5% and 10%, respectively. This threshold is low enough to be called early detection and yet not that low that the faults are not visible in the figures while having a rather strong noise present in the measurements. However, with a proper signal processing tool even smaller faults are detectable. In addition, Having the same ITSC fault severity in all the phases also enables us to see the difference in the residual responses while subject to the same criteria. This also means that higher fault levels are easily detectable using this method. The noise signal $w(t)$ is generated by a dynamic filter as follows [21]:

$$H(s) = \frac{\sqrt{2\beta}}{s + \beta}\sigma_\omega \tag{C.10}$$

The dynamic filter has the random signal $v(t)$ as input and $w(t)$ as output. The signal $v(t)$ has intensity equal to 1, which indicates the noise has a total power equal to 1. Based on the data from our previous experimental studies and measurements, parameters

Table C.2: Parameters of Noise Signals

Symbol	Parameter	Value
σ_i	Variance and of noise added to currents	0.1583
β_i	Constant of noise added to currents	$100,000$
σ_v	Variance of noise added to voltages	0.2
β_v	Constant of noise added to voltages	10
σ_ω	Variance of noise added to angular speed	0.1
β_ω	Constant of noise added to angular speed	10

of different noise signals are extracted. These parameters which specify the noise added to currents, voltages, and angular speed signals of the motor are listed in Table C.2.

The residual responses for the mentioned faults are obtained and shown in Fig. C.7 (a)–(d). Before the faults are applied, the motor is operating in healthy mode ($t = 0 - 0.06s$) and all the residuals remain zero (neglecting the noise) since there is not any difference between the measured signals and the calculated ones used in each residual. When the ITSC fault in phase a is applied, only R_1 is affected and obtains a non-zero value. Since ITSC fault in phase a (faults in f_{R_a}, f_{L_a}) is only observable in R_1 (derived from $MTES_4$), other residuals remain zero when the motor is experiencing this fault. The same logic can be used for R_2 and R_3 as they obtain non-zero values and only these two residuals are affected when ITSC faults in phase-b and phase-c are applied to the motor. Between $t = 0 - 0.06s$ and when the demagnetization fault is applied on the motor, all the residuals obtain a non-zero value. The behavior and response of the residuals during each fault, can be used as the ground for detecting and discriminating of the mentioned faults in the PMSM.

To isolate the faults based on the response of the residuals, a decision-making system is proposed based on logical blocks and added to the diagnostic system. To detect and isolate ITSC fault in phase a, R_1 should be non-zero while other residuals remain zero. For ITSC fault in phase b, R_2 should be non-zero while other residuals remain zero. For detection and isolation of ITSC in phase c, R_3 should be non-zero while other residuals remain zero. When all the four residuals have a non-zero value, it means that the motor is experiencing a demagnetization fault. Fig. C.8 shows the output signal of the decision-making system.

C.5 Conclusion

In this paper, we presented a novel method to detect ITSC and demagnetization faults in the PMSM. Structural analysis is implemented on the mathematical model of the PMSM to detect and isolate the mentioned faults in the system. After obtaining the redundant part of the structural model by employing DM decomposition tool, the system is divided into redundant sub-models called minimal test equation support. Four sequential residuals

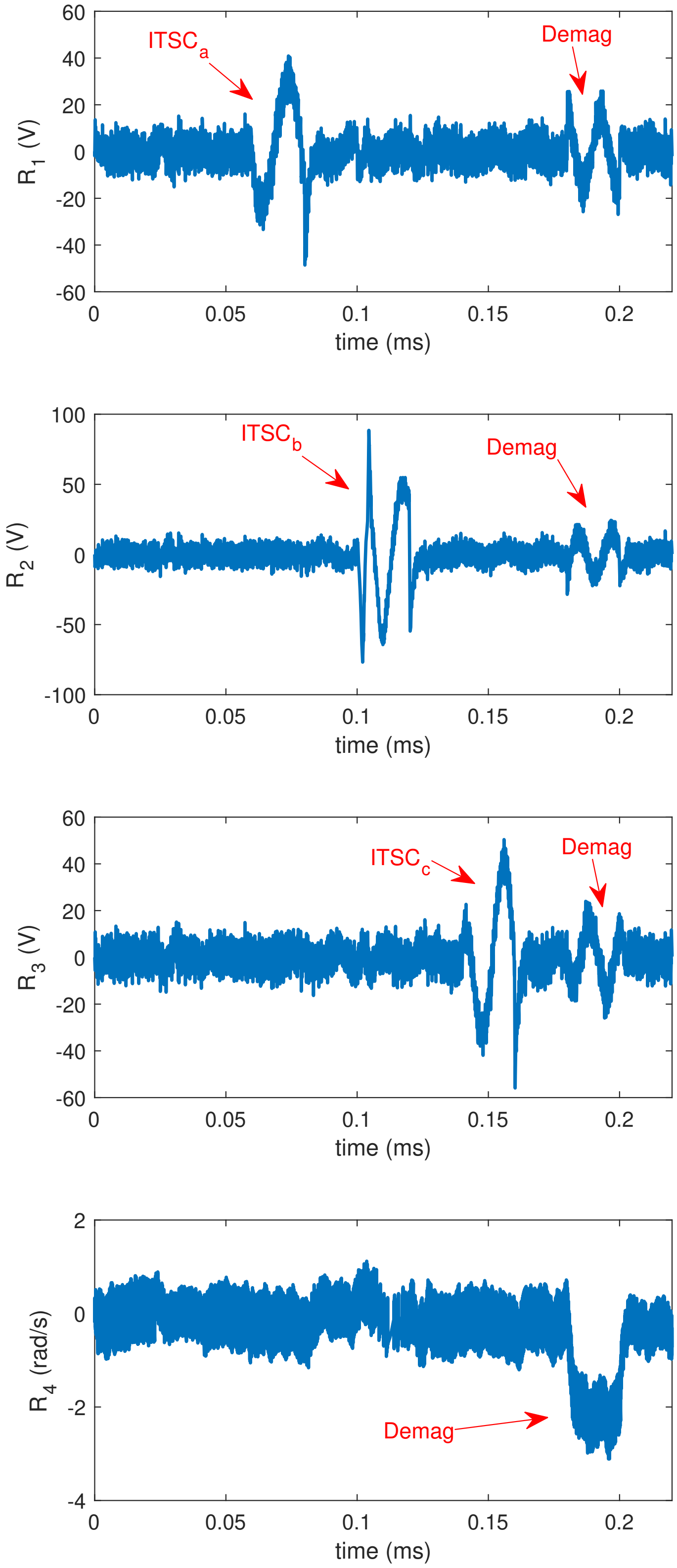

Figure C.7: Response of residuals.

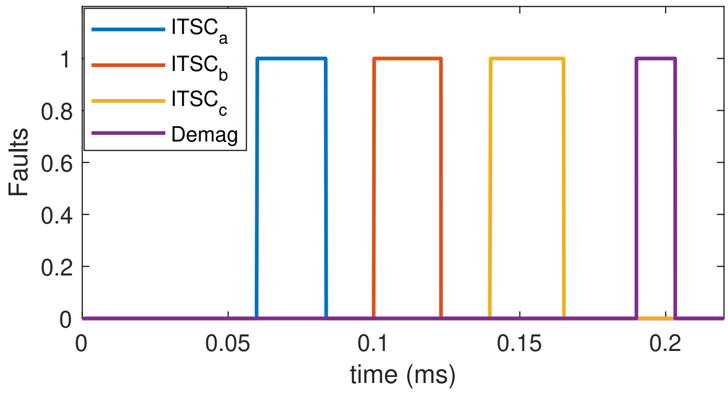

Figure C.8: Discrimination of ITSC and demagnetization faults.

are derived based on the fault terms that appear in each of the MTES sets to detect and isolate four faults in the system including ITSC in phase a, ITSC in phase b, ITSC in phase c, and demagnetization. The proposed model is implemented in Matlab/Simulink and the mentioned faults are applied to the system in different time intervals. The results show that residuals are able to efficiently detect and isolate even small faults in the presence of noise, proving the effectiveness of this diagnostic approach.

References

[1] Seungdeog Choi, Moinul Shahidul Haque, Md Tawhid Bin Tarek, Vamsi Mulpuri, Yao Duan, Sanjoy Das, Vijay Garg, Dan M Ionel, M Abul Masrur, Behrooz Mirafzal, et al. Fault diagnosis techniques for permanent magnet ac machine and drives—a review of current state of the art. *IEEE Transactions on Transportation Electrification*, 4(2):444–463, 2018.

[2] Subhasis Nandi, Hamid A Toliyat, and Xiaodong Li. Condition monitoring and fault diagnosis of electrical motors—a review. *IEEE Transactions on Energy Conversion*, 20(4):719–729, 2005.

[3] Yuan Qi, Emine Bostanci, Vigneshwaran Gurusamy, and Bilal Akin. A comprehensive analysis of short-circuit current behavior in pmsm interturn short-circuit faults. *IEEE Transactions on Power Electronics*, 33(12):10784–10793, 2018.

[4] Bon-Gwan Gu, Jun-Hyuk Choi, and In-Soung Jung. Development and analysis of interturn short fault model of pmsms with series and parallel winding connections. *IEEE Transactions on Power Electronics*, 29(4):2016–2026, 2013.

[5] Martin Riera Guasp, Jose A Antonino Daviu, and Gérard-André Capolino. Advances in electrical machine, power electronic, and drive condition monitoring and fault detection: state of the art. *IEEE Transactions on Industrial Electronics*, 62(3):1746–1759, 2014.

[6] Bo Wang, Jiabin Wang, Antonio Griffo, and Bhaskar Sen. Stator turn fault detection by second harmonic in instantaneous power for a triple-redundant fault-tolerant pm drive. *IEEE Transactions on Industrial Electronics*, 65(9):7279–7289, 2018.

[7] Ehsan Mazaheri-Tehrani, Jawad Faiz, Mohsen Zafarani, and Bilal Akin. A fast phase variable *abc* model of brushless pm motors under demagnetization faults. *IEEE Transactions on Industrial Electronics*, 66(7):5070–5080, 2018.

[8] Hongwen He, Nana Zhou, Jinquan Guo, Zheng Zhang, Bing Lu, and Chao Sun. Tolerance analysis of electrified vehicles on the motor demagnetization fault: From an energy perspective. *Applied Energy*, 227:239–248, 2018.

[9] Zhi Yang, Xiaodong Shi, and Mahesh Krishnamurthy. Vibration monitoring of pm synchronous machine with partial demagnetization and inter-turn short circuit faults. In *2014 IEEE Transportation Electrification Conference and Expo (ITEC)*, pages 1–6. IEEE, 2014.

[10] J Urresty, J Riba, L Romeral, and H Saavedra. Analysis of demagnetization faults in surface-mounted permanent magnet synchronous with inter-turns and phase-to-ground short-circuits. In *2012 XXth International Conference on Electrical Machines*, pages 2384–2389. IEEE, 2012.

[11] Hojin Lee, Hyeyun Jeong, and Sang Woo Kim. Detection of interturn short-circuit fault and demagnetization fault in ipmsm by 1-d convolutional neural network. In *2019 IEEE PES Asia-Pacific Power and Energy Engineering Conference (APPEEC)*, pages 1–5. IEEE, 2019.

[12] Hyeyun Jeong, Hojin Lee, and Sang Woo Kim. Classification and detection of demagnetization and inter-turn short circuit faults in ipmsms by using convolutional neural networks. In *2018 IEEE Energy Conversion Congress and Exposition (ECCE)*, pages 3249–3254. IEEE, 2018.

[13] Seokbae Moon, Hyeyun Jeong, Hojin Lee, and Sang Woo Kim. Detection and classification of demagnetization and interturn short faults of ipmsms. *IEEE Transactions on Industrial Electronics*, 64(12):9433–9441, 2017.

[14] Shen Zhang and Thomas G Habetler. Transient demagnetization characteristics of interior permanent magnet synchronous machines with stator inter-turn short circuit faults for automotive applications. In *2018 IEEE Energy Conversion Congress and Exposition (ECCE)*, pages 1661–1667. IEEE, 2018.

[15] Kyung-Tae Kim, Yoon-Seok Lee, and Jin Hur. Transient analysis of irreversible demagnetization of permanent-magnet brushless dc motor with interturn fault under the operating state. *IEEE Transactions on Industry Applications*, 50(5):3357–3364, 2014.

[16] Jiyu Zhang, Hongyang Yao, and Giorgio Rizzoni. Fault diagnosis for electric drive systems of electrified vehicles based on structural analysis. *IEEE Transactions on Vehicular Technology*, 66(2):1027–1039, 2016.

[17] Mattias Krysander, Jan Åslund, and Mattias Nyberg. An efficient algorithm for finding minimal overconstrained subsystems for model-based diagnosis. *IEEE Transactions on Systems, Man, and Cybernetics-Part A: Systems and Humans*, 38(1):197–206, 2007.

[18] Mattias Krysander and Erik Frisk. Sensor placement for fault diagnosis. *IEEE Transactions on Systems, Man, and Cybernetics-Part A: Systems and Humans*, 38(6):1398–1410, 2008.

[19] Carl Svärd, Mattias Nyberg, Erik Frisk, and Mattias Krysander. Automotive engine fdi by application of an automated model-based and data-driven design methodology. *Control Engineering Practice*, 21(4):455–472, 2013.

[20] Christofer Sundström, Erik Frisk, and Lars Nielsen. Selecting and utilizing sequential residual generators in fdi applied to hybrid vehicles. *IEEE Transactions on Systems, Man, and Cybernetics: Systems*, 44(2):172–185, 2013.

[21] Mogens Blanke, Michel Kinnaert, Jan Lunze, and Marcel Staroswiecki. Diagnosis and fault tolerant control, 2016.

[22] Mattias Krysander. *Design and analysis of diagnosis systems using structural methods*. PhD thesis, PhD thesis, Linköping Univ., Linköping, Sweden, 2006.

[23] Mattias Krysander, Jan Åslund, and Erik Frisk. A structural algorithm for finding testable sub-models and multiple fault isolability analysis. In *21st International Workshop on Principles of Diagnosis (DX-10), Portland, Oregon, USA*, pages 17–18, 2010.

[24] Saeed Hasan Ebrahimi, Martin Choux, et al. Modeling stator winding inter-turn short circuit faults in pmsms including cross effects. In *2020 International Conference on Electrical Machines (ICEM)*, volume 1, pages 1397–1403. IEEE, 2020.